Bioelectrochemistry 134 (2020) 107524

Contents lists available at ScienceDirect

Bioelectrochemistry

journal homepage: www.elsevier.com/locate/bioelechem

From algal cells to autofluorescent ghost plasma membrane vesicles

Nadica Ivošević DeNardis [a,*], Galja Pletikapić [a], Ruža Frkanec [b], Lucija Horvat [a], P. Thomas Vernier [c]

[a] Ruđer Bošković Institute, Zagreb, Croatia
[b] Centre for Research and Knowledge Transfer in Biotechnology, University of Zagreb, Croatia
[c] Frank Reidy Research Center for Bioelectrics, Old Dominion University, Norfolk, VA, USA

ARTICLE INFO

Article history:
Received 15 November 2019
Received in revised form 25 March 2020
Accepted 27 March 2020
Available online 30 March 2020

Keywords:
Algal cell
Autofluorescent ghost vesicle
Calcein
Dunaliella tertiolecta
GUV
Membrane permeability

ABSTRACT

Plasma membrane vesicles can be effective, non-toxic carriers for microscale material transport, provide a convenient model for probing membrane-related processes, since intracellular biochemical processes are eliminated. We describe here a fine-tuned protocol for isolating ghost plasma membrane vesicles from the unicellular alga *Dunaliella tertiolecta*, and preliminary characterization of their structural features and permeability properties, with comparisons to giant unilamellar phospholipid vesicles. The complexity of the algal ghost membrane vesicles reconstructed from the native membrane material released after hypoosmotic stress lies between that of phospholipid vesicles and cells. AFM structural characterization of reconstructed vesicles shows a thick envelope and a nearly empty vesicle interior. The surface of the envelope contains a heterogeneous distribution of densely packed, nanometer-scale globules and pore-like structures which may be derived from surface coat proteins. Confocal fluorescence imaging reveals the highly pigmented photosynthetic apparatus located within the thylakoid membrane and retained in the vesicle membrane. Transport of the fluorescent dye calcein into ghost and giant unilamellar vesicles reveals significant differences in permeability. Expanded knowledge of this unique membrane system will contribute to the design of marine bio-inspired carriers for advanced biotechnological applications.

1. Introduction

For many years model systems constructed from simple phospholipids have been used to study membrane structure and function [1,2]. More recently, methods for preparing phospholipid membranes with anchored and embedded components have been developed to mimic more closely cell–cell interactions, surface recognition, and targeted drug delivery [3–8]. None of these systems, however, approaches the complexity of cell membranes.

Exosomes are higher complexity systems consisting of a lipid bilayer with bound proteins and nucleic acids. These nanometer-sized extracellular membrane vesicles are secreted by eukaryotic cells in culture as a mode of intercellular communication. The molecular mechanism of their formation is not completely understood and detection and analysis are challenging [9,10].

Seeking a physiologically relevant membrane model from aquatic systems that would closely mimic the cell membrane, and in such a way to link the ocean and human health, is a highly competitive field for pharmaceutical companies [11,12]. Algae are a source of food, pharmacological agents, and energy [13–15], and their potential is underexplored. Algae are exploited for the extraction of valuable bioactive compounds – pigments, glycerol, fatty acids [15] – and thus they are biotechnologically relevant. There is great interest in culturing microalgae in open pond systems for biofuel production, but economic feasibility is uncertain [16,17]. Another possible application is an algae-powered bioreactor for oxygen production and as super-food for astronauts at the space station [18,19].

Unicellular green flagellate algae of the genus *Dunaliella* are widespread in marine and freshwater systems [15]. *Dunaliella tertiolecta* is a halotolerant, euryhaline organism found in marine environments. The lack of a rigid cell wall, leaving only a glycocalyx-type cell envelope, enables the use of *Dunaliella* species as model organisms for osmoregulation studies, toxicity assays [20], and for the isolation of plasma membrane vesicles.

D. tertiolecta cells have been imaged at high resolution, and nanomechanical properties were determined during two phases of their growth (exponential vs. stationary) [21]. Algal cell hydrophobicity was determined by chemical force measurements with AFM tips functionalized with $-CH_3$ groups. AFM results revealed that algal cells were significantly stiffer and more hydrophobic in exponential than in the stationary phase suggesting a molecular modification of the cell envelope during the aging

* Corresponding author.
E-mail address: ivosevic@irb.hr (N. Ivošević DeNardis).

https://doi.org/10.1016/j.bioelechem.2020.107524
1567-5394/

process. On the other hand, increased *Dunaliella* cell stiffness may be the consequence of adaptation to heavy metal-induced stress [22].

Possibilities for exploitation of isolated algal ghost membranes have not been explored. In Jokela's analysis of isolated *Dunaliella* cell envelopes using sucrose gradient centrifugation, chemical characterization revealed relatively high hydrophobic amino acid content [23]. The aim of this study is to fine-tune a protocol for isolating ghost plasma membrane vesicles from the unicellular alga *Dunaliella tertiolecta*, and to provide preliminary characterization of their structural features and permeability properties, with comparisons to giant unilamellar phospholipid vesicles.

2. Materials and methods

2.1. Cell suspensions

The unicellular marine algae *Dunaliella tertiolecta* Butcher (Chlorophyceae) [Culture Collection, Bigelow Laboratory for Ocean Sciences] was cultured in seawater enriched with F-2 medium [24] under ambient conditions (18 °C, 12 h light:12 h dark). Cell density was 2×10^6 cells/mL after 19 days of growth. The cells (long dimension 6–12 μm) were separated from the growth medium by mild centrifugation (1500 *g*, 5 min). The loose pellet was washed several times with filtered seawater by centrifugation. Stock suspension contained $1–6 \times 10^7$ cells/mL.

2.2. Isolation of algal ghost vesicles

Algal ghost vesicles were produced by the osmotic shock of the photosynthetic marine microalga *Dunaliella tertiolecta* by centrifugation and without the use of sucrose in order not to modify ghost vesicle surface properties. Schematic 1 shows the isolation protocol.

Due to the fragile nature of ghost vesicles, the sample must be carefully handled. The vesicle yield rate depends on the growth phase of the cell culture. The highest yield was obtained from cells in the early stationary phase (19 days of culture). To begin ghost vesicle preparation, a loose algal cell pellet is isolated from 500 mL of cell growth medium by mild centrifugation (1500 *g* for 5 min) and rinsing with the filtered seawater (0.22 μm) as described under Section 2.1. The supernatant was completely removed, and 4 mL of the loose algal cell pellet was diluted 40 times with ultrapure water, vigorously shaken on a vortex, and then left at room temperature. After 30 min, samples are centrifuged at 1500 *g* for 4 min. The Pellet 1 contains released intracellular material, half-emptied vesicles, and some empty vesicles. Supernatant 1, which contains empty ghost vesicles, vesicles with some attached material, and a small amount of free debris, is centrifuged at 15,000 *g* for 15 min. The resulting Pellet 3 contains mainly debris and some vesicles, while Supernatant 3 contains mostly empty ghost vesicles and ghost vesicles with some attached material, concentrated in a thin, viscous layer above Pellet 3. Tris buffer concentration of 10 mM containing 10 mM $MgCl_2$ and pH 7.4 was used throughout the experiments with algal ghost vesicles. The 3 mL of viscous solution is carefully aspirated with a micropipette and resuspended in 3 mL of 10 mM Tris buffer containing 10 mM $MgCl_2$ (Mg^{2+} stabilizes the vesicles when introduced after the ghosts are formed). Tris buffer is preferable to HEPES, which causes a decrease in ghost vesicle size and concentration. The final concentration of ghost vesicles in suspension is ~10^4 vesicles/mL. Further centrifugation of Supernatant 3 to remove remaining debris could cause ghost vesicle loss.

If the yield of ghost vesicles in Supernatant 3 is not sufficient, Pellet 1 should be used for vesicle isolation. Pellet 1 is resuspended in 50 mL of 10 mM Tris buffer containing 10 mM $MgCl_2$ and centrifuged at 1000 *g* for 5 min, according to the protocol depicted in Schematic 1.

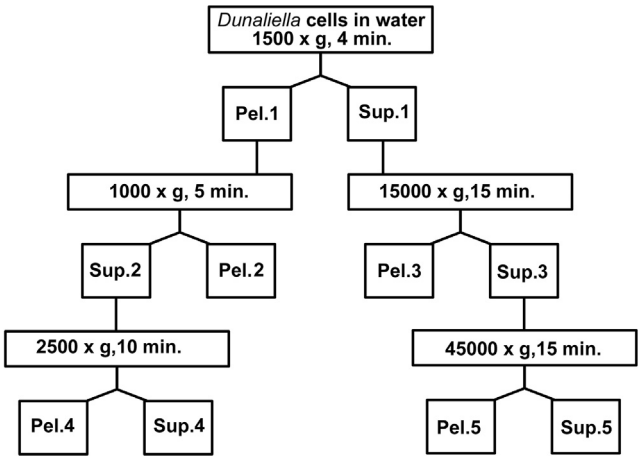

Schematic 1. Isolation protocol of algal ghost vesicle.

2.3. GUV preparation

1,2-dioleoyl-*sn*-glycero-3-phosphocholine (DOPC, 99%) was from Sigma-Aldrich (St. Louis, MO, USA) and used as received. HEPES (2-[4-(2-hydroxyethyl)-1-piperazinyl]-ethanesulfonic acid was purchased from Merck, Darmstadt, Germany. HEPES buffer concentration of 10 mM and pH 7.4 was used throughout the experiments with giant unilamellar vesicles. Calcein was from Sigma-Aldrich. A solution of 80 mM calcein prepared by dissolving calcein in 1 M KOH was diluted to 20 mM in 1 M HEPES buffer for a working stock solution. The final concentration of calcein used in experiments was 200 μM in 10 mM HEPES buffer.

Giant unilamellar vesicles (GUV) were prepared by reverse-phase evaporation as previously described [25]. Briefly, DOPC was dissolved in a mixture of chloroform: methanol (2 μmol, 2.54 mg DOPC in 1 mL chloroform and 200 μL MeOH, 1.67 M) and the solution was transferred to a 50 mL round-bottom flask. The aqueous phase, 7 mL of 10 mM HEPES buffer, pH 7.4, was then carefully added. The organic solvent was removed in a rotary evaporator (Buchi Rotavapor RE 121, Buchi Water bath 461 and Buchi Vacuum Pump V-710) under pressure of 5 kPa and at 48 °C. After evaporation for several minutes, an opalescent fluid containing GUVs was obtained. GUVs containing calcein were prepared by the same procedure except that calcein was added to the HEPES buffer (final concentration 200 μM calcein) before evaporation of the organic solvent. GUVs were separated from non-encapsulated calcein by centrifugation (Eppendorf centrifuge 5810 R) at 3220 *g* for 1 h. Supernatants were removed and vesicle pellets resuspended in 300 μL 10 mM HEPES buffer.

2.4. Epifluorescence and confocal microscopy

A fluorescence microscope Olympus BX 51 was used to examine cell viability, densities, and to monitor the ghost vesicle isolation process. Confocal measurements were performed on a Leica TCS SP8 laser scanning confocal microscope equipped with a white light laser, using a 63× (N.A. = 1.4) oil-immersion objective. Excitation and emission spectra generated by the microscope were used to optimize the emission windows. For better visualization of the cells and vesicles, two commercial dyes were used: the lipophilic membrane stain DiI (excitation maximum 552 nm, detection range 570–600 nm), and the actin probe SiR-actin (excitation maximum 650 nm, detection range 700–730 nm). For detection of electroper-

meabilization, the fluorescent dye calcein was used (excitation maximum 488 nm, detection range 500–540 nm).

2.5. Sample preparation for confocal imaging

Before use, the coverslip was washed with ethanol and rinsed with water. When dried, 50 μL polyethylenimine PEI (0.5%) was added on the coverslip and left in contact for 30 min, followed with the rinsing of the coverslip with water. 50 μL of cell aliquot is placed on the modified coverslip and left in contact for 30 min. Non-attached cells were washed with filtered seawater (0.22 μm) [21]. SiR-actin Kit (50 nmol SiR-actin, 1 μmol Verapamil) was purchased from Tebu-Bio SAS. The stock concentration of SiR-actin of 500 μM was prepared in DMSO solution. The stock solution of SiR-actin was 1000 times diluted in cell and vesicle suspensions before measurements. The samples were labeled with DiI with the final concentration of 2 μM.

2.6. Sample preparation for AFM measurements

For AFM imaging, a 5 μL volume of the suspension containing plasma membrane vesicles was pipetted directly onto freshly cleaved mica and allowed to dry for 30 min in an enclosed Petri dish before imaging. AFM imaging of vesicles was performed using a MultiMode Scanning Probe Microscope with a Nanoscope IIIa controller (Bruker, Billerica USA) with a vertical engagement (JV) 125 μm scanner. Images were recorded in contact mode using a standard silicon nitride tip (NP-20, Bruker, nominal frequency 56 kHz, nominal spring constant of 0.32 $N{\cdot}m^{-1}$) with a scan resolution of 512 samples per line. Scanning rates were normally optimized around 1–2 Hz. Processing and analysis of images were carried out using the NanoScopeTM software (Digital Instruments, Version V614r1, and V531r1). The force was kept at the lowest possible value to minimize the forces of interaction between the tip and the surface. Measurements were performed in air, at room temperature and 50–60% relative humidity, which leaves the samples with a small hydration layer, helping to maintain the structure [26]. All images are presented as raw data except for the first-order two-dimensional flattening.

2.7. Electropermeabilization

Electropermeabilization of GUVs resuspended in 10 mM HEPES buffer was performed in electroporation cuvettes (Eppendorf, 1 mm gap, 100 μL volume), with electric field 80 kV/m, number of pulses 100, pulse duration 1 ms, using Gene Pulser Xcell (Bio Rad Laboratories, Inc). Electric pulses were delivered to samples in standard electroporation cuvettes with a commercial electroporation instrument, which has monitoring and protection circuits for current and voltage. No error conditions were detected. The pulse duration, amplitude, and repetition rate come from standard protocols for which it has been established that there is no significant heating of the samples.

3. Results

3.1. Imaging of algal ghost vesicles

Fig. 1 shows representative optical micrographs of *D. tertiolecta* cells before (left panel) and after exposure to the hypoosmotic shock showing in the middle panel the ghost vesicles with released intracellular material and in the right panel a dense suspension of mainly empty ghost vesicles with the corresponding size distribution plot.

D. tertiolecta cells range from 6 to 12 μm long. Algal ghost vesicles are mainly spherical, ranging in diameter from 3 to 30 μm. They are stable for up to two weeks when stored at 4 °C.

Representative confocal images of an algal cell and ghost vesicle (fluorescence, white light, and overlays) in Fig. 2 show autofluorescence of the algal cell body and lack of fluorescence in the flagellar body region.

Ghost autofluorescence is confined to the vesicle perimeter. Autofluorescence spectra of an algal cell and ghost vesicle, obtained with the Lambda-Scan option of the Leica TCS SP8, are presented in Fig. 3.

Two excitation wavelengths, 490 nm and 660 nm produce emission peaking in the range 630–750 nm. When excited with 490 nm, ghost vesicles, but not cells, show a second, weaker emission peak in the range 495–550 nm. The red emission wavebands (630–750 nm) are most likely chlorophyll fluorescence [27], which is expected in intact cells, and probably is due to residual chlorophyll in ghost vesicles. The yellow emission (495–550 nm) might be due to carotenoids, a known component of *D. tertiolecta* pigments [28,29]. In the algal photosystem, carotenoids are mostly membrane-bound, but algal carotenoid fluorescence in solutions [30], as well as in live algal cells [31], has been demonstrated. Fig. 4 compares confocal images of a SiR-actin-stained *D. tertiolecta* cell and ghost vesicle.

Actin filaments are densely distributed in the algal cell body but not in the flagellar region. On the other hand, actin filaments are associated only with the ghost membrane; the vesicle interior shows no actin network. In some cases, DiI and SiR-actin staining reveal a ghost vesicle surrounded by a cloud of lipid material, most likely endoplasmic reticulum and other intracellular membrane extruded from the cell by the hypoosmotic shock [32,33].

A topographic image of a representative algal ghost recorded in air is shown in Fig. 5.

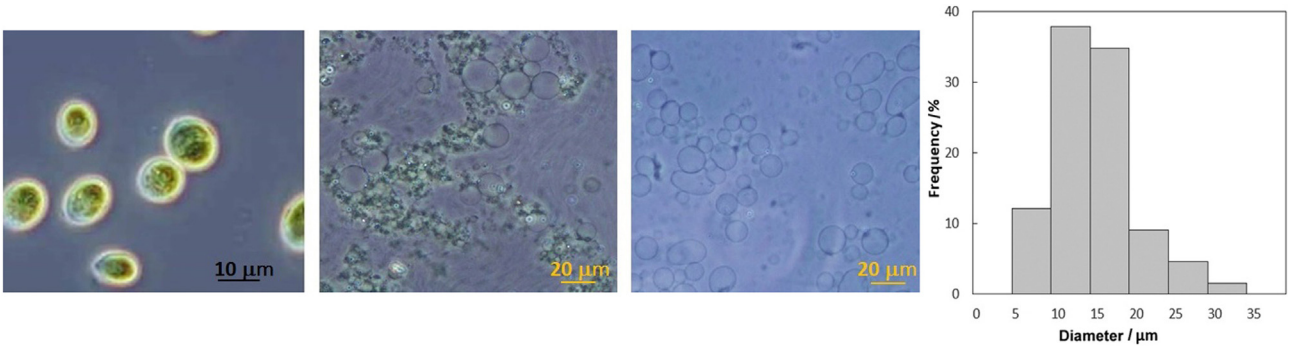

Fig. 1. Representative optical micrographs of *D. tertiolecta* cells before (left panel) and after exposure to the hypoosmotic shock showing in the middle panel the ghost vesicles with released intracellular material and in the right panel a dense suspension of mainly empty ghost vesicles with the corresponding size distribution plot.

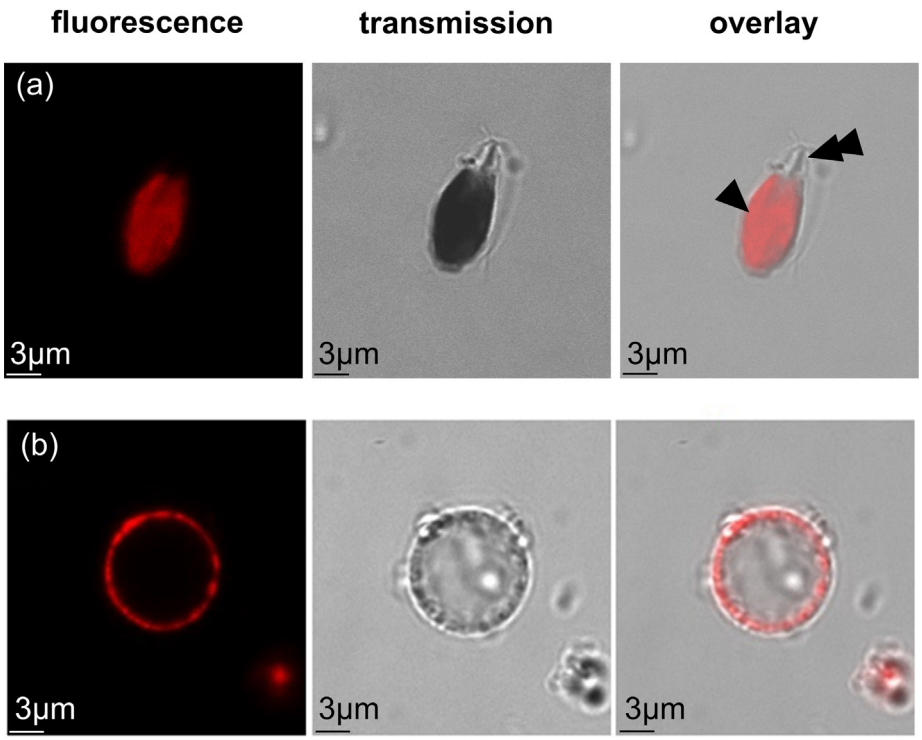

Fig. 2. Representative confocal images of individual *D. tertiolecta* cell and ghost vesicle under fluorescence, transmission mode, and corresponding overlaid image.

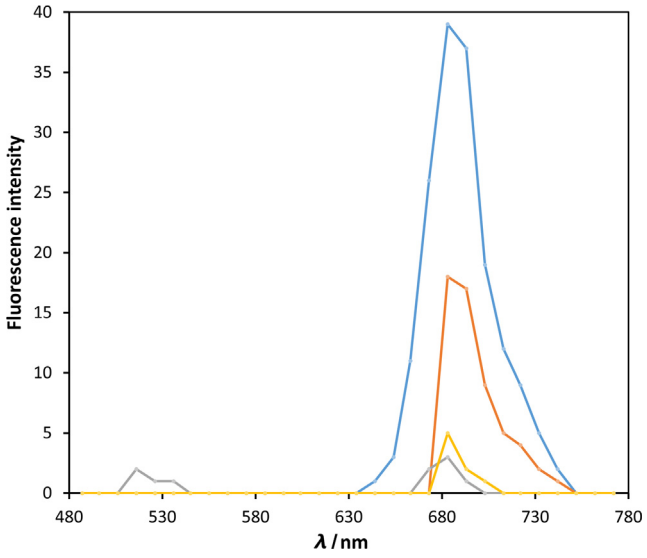

Fig. 3. Overlapped autofluorescence spectra of the algal cell and algal ghost vesicle, excitation 490 nm (blue line-*D. tertiolecta* cell, grey line-algal ghost vesicle) and 690 nm (orange line-*D. tertiolecta* cell, yellow line-algal ghost vesicle).

The average thickness of the deflated part of vesicles is 20 nm, suggesting that the thickness of the cell envelope is 10 nm, in agreement with an early electron micrograph [23]. Magnification of the topographic scan shows a heterogeneous distribution of densely packed globules ranging from 5 to 15 nm in height, forming pore-like structures of nanometer size.

3.2. Permeability of algal ghost vesicles

Algal ghost vesicle membranes are permeable to the anionic fluorescent dye calcein, rapidly equilibrating (<3 min) intravesicular and extravesicular calcein concentrations when placed in 200 μM calcein. In a typical sample about 90% of the ghosts are immediately filled while the remainder equilibrate more slowly (Fig. 6).

The same permeability to calcein was observed when calcein-loaded ghost vesicles were placed in buffer containing no calcein. The vesicles quickly became nonfluorescent as the calcein diffused into the external medium.

We examined two approaches to annealing the ghost membranes (to make them less permeable). Adding 5 mM or 10 mM of calcium one minute after the hypoosmotic shock had little effect, even if the ghost vesicle suspension was incubated for a few minutes at 37 °C. We also tried the nonionic block linear copolymer (Poloxamer 188), which can stabilize and seal plasma membranes via direct incorporation into the phospholipid bilayer [34]. Suspending ghost vesicles in 25 mM Polaxomer 188 in 10 mM Tris buffer with 200 μM calcein (and without $MgCl_2$) slowed entry of calcein into the vesicles (many vesicles still exclude calcein after 10 min).

3.3. Permeability of GUV (DOPC)

For comparison, we examined the permeability to calcein of GUVs prepared from the zwitterionic phospholipid DOPC. Fig. 7a and b show the empty GUVs stained with DiI in calcein solution before and after exposure to electrical stress.

Calcein was added to the GUV suspension 15 min before electrical stress and imaging. The unstressed GUVs are impermeable to calcein (no change in fluorescence inside of vesicle). Electrical stress permeabilizes the GUVs, indicated by the entry of the fluorescent calcein into the vesicles. Fig. 7c and d show calcein-loaded GUVs before and after exposure to electrical stress. When the same (or stronger) permeabilizing electrical field used above was applied to provoke calcein release, no fluorescence change was detected, indicating a failure to produce a persistent permeabilization of the calcein-loaded vesicles. As a positive control, treatment of calcein-loaded GUVs with the nonionic surfactant

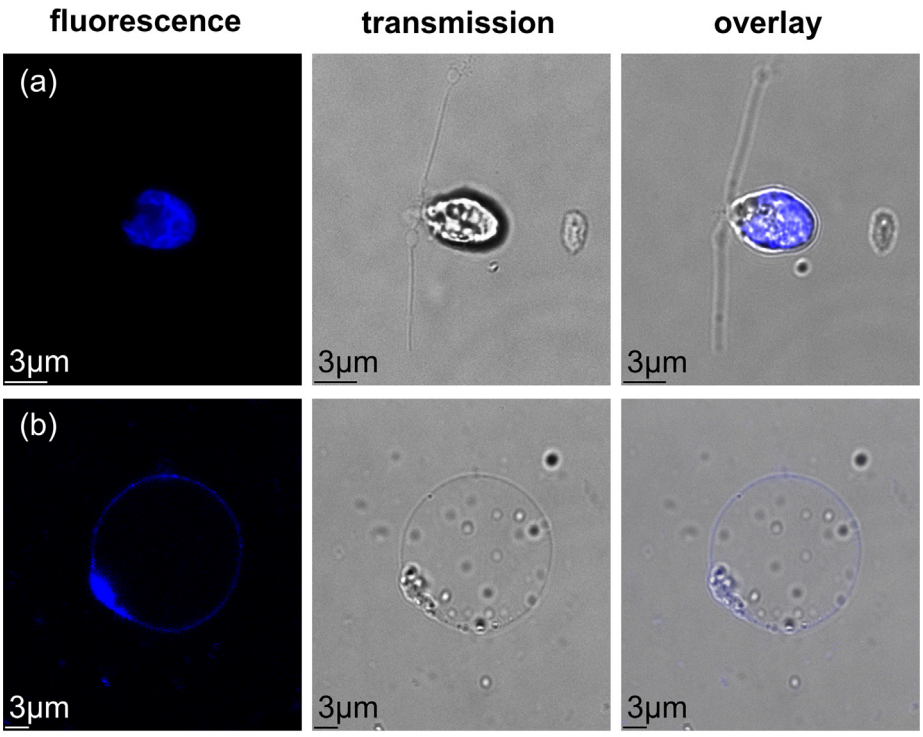

Fig. 4. Representative confocal images of individual *D. tertiolecta* cell and algal ghost vesicle stained with SiR-actin under fluorescence, transmission mode, and corresponding overlaid image.

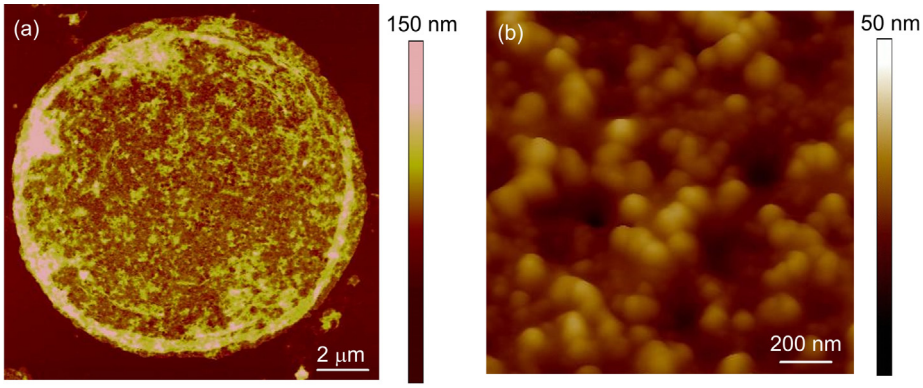

Fig. 5. AFM images of typical ghost vesicle enlarged membrane areas (a) and representative membrane area at high resolution showing globule like morphology (b).

Triton-X-100 (0.1%) caused vesicle permeabilization and an equilibration of intra- and extravesicular calcein concentrations.

4. Discussion

The lack of a rigid cell wall and the associated low stiffness of the cells (stiffness of *D. tertiolecta* [21,22] is comparable to that of red blood cells) facilitate the isolation of ghost vesicles from *D. tertiolecta* by osmotic stress. Ghost vesicles cannot be isolated by osmotic shock from algal cells possessing a rigid cell wall, which are significantly stiffer [26].

The *Dunaliella* cell "coat" (glycocalyx) appears to be made up of glycoproteins of ~150 kDa existing in an outer layer surrounding the cell, demonstrated by staining with cationic dyes [35]. The cell envelope, including the plasma membrane, is around 9 nm thick [23,36].

AFM images reveal that the surface of *Dunaliella* ghost membranes is densely packed with globular forms with height ranging from 5 to 15 nm, assembled in pore-like structures which could contribute to the permeability of the vesicle. Based on the proteome profile of the related *D. salina*, these globular structures probably correspond to surface coat proteins, lipid-metabolizing enzymes, ion transporters, GTP-binding proteins, heat shock proteins and other membrane proteins of unknown function [15,37]. Isolated algal ghost membrane is naturally labeled due to the pigmented photosynthetic apparatus located within the thylakoid membrane [38].

The predominant constituents of the isolated cell envelopes are proteins (84%) and phospholipids (14%) [23]. Because of their high nutritional value (proteins, lipids, carbohydrates), microalgae are extensively used as a source of food [39]. The high-protein content microalga *Chlorella* was found to enhance the growth of intestinal Lactobacillus, while *Spirulina sp*. and *Dunaliella* sp. can act as potent anti-cancer agents due to their carotenoid content.

The cell membrane fraction is characterized by a high phosphatidic acid content, important for membrane fusion, its dependence

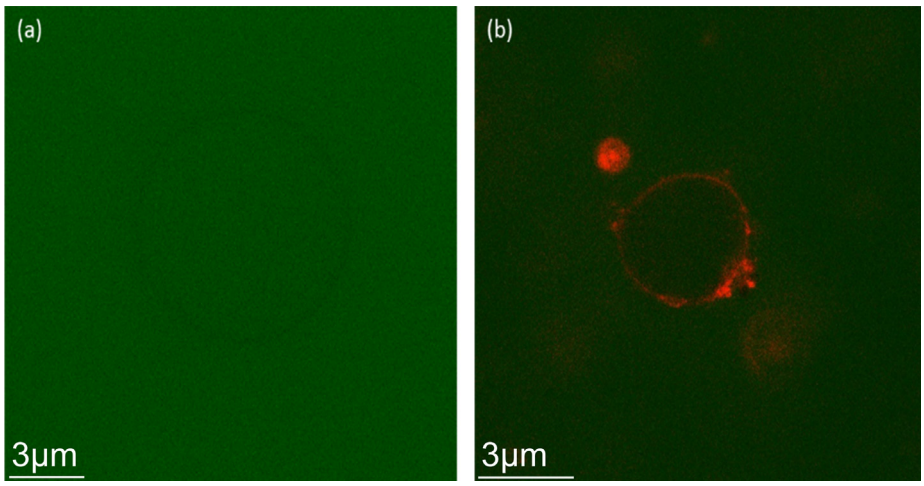

Fig. 6. Typical confocal images of calcein-loaded algal ghost vesicles before (a) and after staining of the membrane with DiI.

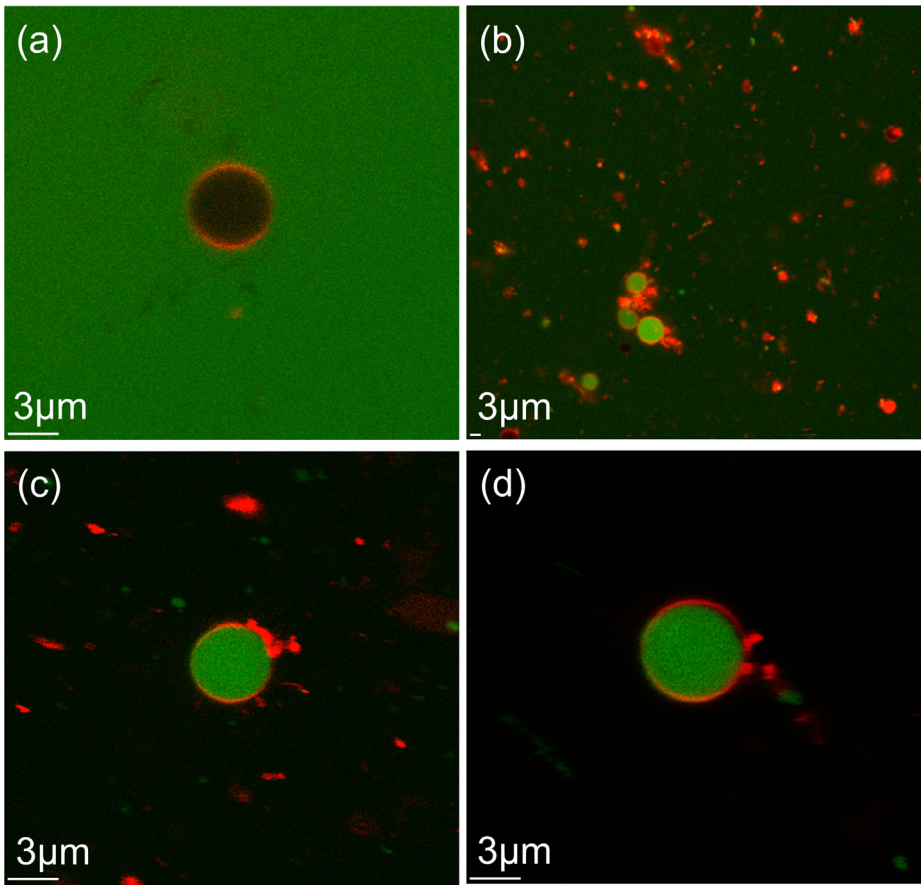

Fig. 7. Typical confocal images of: (i) empty GUV in calcein buffer solution before (a) and after application of electrical stress (b), calcein-loaded GUV before (c) and after the application of electrical stress (d). DiI-stained membranes.

on divalent ions for stability, the high fraction of hydrophobic amino acids, and the presence of the Na^+-K^+- ATPase. Predominant fatty acids are palmitic and linolenic, with lesser amounts of oleic, stearic, and linoleic residues [23,40].

Numerous studies have utilized fluorescent dyes as indicators of membrane electropermeabilization (electroporation) [41–45]. Calcein is a hydrophilic, anionic, natively fluorescent dye widely used as a membrane-impermeant compound in cell studies and for investigating mechanisms for the release of incorporated content from lipid vesicles. Neumann and coworkers interpreted electroporative dye transport in mouse lymphoma cells in terms of the kinetics of electropore formation and resealing, and the transport of dye through the porated membrane [46]. Recently a quantitative comparison of the transport of three similarly sized but chemically different fluorescent indicators – YO-PRO-1, propidium, and calcein – into permeabilized cells showed strikingly different patterns of entry, where the charge of the molecules plays an important role [47,48]. The influx of YO-PRO-1 and propidium (cations) is much

greater than the influx of calcein (anion), but the ***efflux*** of calcein from pre-loaded cells into the medium after electropermeabilization is roughly equivalent to the ***influx*** of YO-PRO-1 and propidium. Our preliminary data shows undetectable uptake of calcein into intact and electropulsed *D. tertiolecta* cells, but autofluorescence signals complicate the interpretation of these results.

The ghost vesicles, however, are spontaneously permeable to calcein. The *Dunaliella* cell membrane itself seems to be naturally porous, which enables the fast release of glycerol or other metabolites, an adaptive response to osmotic stress [15]. The greater permeability of the ghost membrane might indicate that healing of the membrane did not occur completely after ghost isolation, or some active uptake mechanism may exist. The relatively high fraction of protein in algal ghost membrane increases the possibility that proteins play a role in calcein transport through ghost membrane.

The properties of *Dunaliella* ghost vesicles may be qualitatively compared with those of artificial phospholid vesicles. Giant unilamellar vesicles, a well-recognized simple membrane model, can serve as a framework for understanding the results obtained with more complex system of plasma membrane vesicles. Giant unilamellar vesicles are cell-sized, characterized by low curvature, controllable tension, and large surface [49,50]. The unique composition of algal plasma membrane vesicles may be better elucidated through comparisons with GUVs of specific lipid composition, mimicking membrane fluidity under specific experimental conditions. DOPC GUVs are much less permeable to calcein than are the ghost vesicles (Figs. 6 and 7). The Young's modulus of egg phosphotidylcholine (PC) vesicles is in the range of 2 MPa, about 2 orders of magnitude higher than the algal ghost membranes [51]. The large stiffness of the GUVs is consistent with the two times slower adhesion kinetics of GUVs at the model charged electrode interface compared to the algal ghost vesicle [36,52,53]. Calcein loading into empty GUVs can be accomplished with pulsed electric fields (electroporation), resulting in increased intravesicular fluorescence and a decrease in vesicle size. In a related study, vesicle size decrease and lipid tubular formation were observed due to the pulsed electric field stress of GUV of egg PC [54].

On the other hand, electroporation did not seem to affect vesicles loaded with calcein during vesicle preparation. Vesicle impermeable behavior as shown in Fig. 7d could be supported with the following: (i) Raman spectroscopy confirms that the negatively charged calcein molecules can associate with liposome at their surface through hydrogen bonding interaction between the carboxylate groups of calcein and the polar head groups of liposome which could contribute to membrane reinforcement [44,45,55], (ii) higher interfacial tensions of calcein-loaded GUV vs. empty GUV, since addition of Triton-X-100 caused fluorescence release in background and (iii) vesicle membrane reseals very quickly (nanoseconds) after the porating pulse ends; vesicles do not show persistent permeabilization like cells do. Maherani and coworkers reported different behavior where calcein permeates through the complex liposomal membrane without disruption as evaluated based on the first-order kinetics by using spectrofluorometer. The result shows that the release rate of calcein from liposomes depends on liposome composition, the number, and fluidity of bilayers and its mechanical/physical properties, preparation protocol, and chemo-structural properties of dye [44].

A method for sealing reconstructed algal ghost membranes, which would consequently cause a change in the membrane mechanical properties [56], would be of great interest and would increase the attractiveness of these vesicles as a candidate for transport vehicles. Several groups have reported different approaches for membrane sealing with cross-linking agents such as dinitro-difluorobenzene [23], polymerizing an actin network inside vesicles [57], and composite gel-filled vesicles [58].

5. Conclusions

Algal cells of *D. tertiolecta* represent a practical and potentially valuable source of algal ghost vesicles, for which a preparatory procedure is given here. Algal ghost vesicles are a reconstructed natural system that closely mimics cell membranes in protein, phospholipid, and carbohydrate composition, and in size. Algal ghost vesicles are naturally labeled by the pigmented photosynthetic apparatus located within the thylakoid membrane. Confocal fluorescence imaging reveals actin filaments distributed in the membrane and not in the vesicle interior. The present study represents a first, qualitative attempt to examine algal ghost membrane permeability. The natural ghost membrane is highly permeable for calcein, in contrast to the relative impermeability of artificial DOPC GUVs. The algal ghost vesicle system presents a relevant and convenient model of a photosensitive interface for probing membrane-related processes. The algal ghost membrane is a promising system, a method for sealing ghost vesicles using cross-linking agents and investigate their permeability to a range of fluorescent indicators could open a new avenue toward the use of marine-bio-inspired materials for the development of a new generation of drug delivery systems.

Declaration of Competing Interest

The authors declare that they have no known competing financial interests or personal relationships that could have appeared to influence the work reported in this paper.

Acknowledgments

This work is supported by the Croatian Science Foundation Projects "From algal cell surface properties to stress markers for aquatic ecosystems" (IP-2018-01-5840) and "Synthesis of Supramolecular Self-assembled Nanostructures for Construction of Advanced Functional Materials" (IP-2018-01-6910). PTV is supported by the United States Air Force Office of Scientific Research (AFOSR) grant FA9550-14-1-0023 (a collaborative effort with FA9550-14-1-0018) and by AFOSR MURI grant FA9550-15-1-0517 on "Nanoelectropulse-Induced Electromechanical Signaling and Control of Biological Systems", administered through Old Dominion University.

References

[1] E. Sackmann, A.-S. Smith, Physics of cell adhesion: Some lessons from cell-mimetic systems, Soft Matter 10 (2014) 1644–1659. http://dx.doi.org/10.1039/c3sm51910d.
[2] C. Siontorou, G.-P. Nikoleli, D. Nikolelis, S. Karapetis, Artificial lipid membranes: Past, present and future, Membranes 7 (2017) 38–62, https://doi.org/10.3390/membranes7030038.
[3] V.P. Torchilin, Recent advances with liposomes as pharmaceutical carriers, Nat. Rev. Drug. Discov. 4 (2005) 145–160. http://dx.doi.org/10.1038/nrd1632.
[4] S. Mashaghi, T. Jadidi, G. Koenderink, A. Mashaghi, Lipid Nanotechnology, Int. J. Mol. Sci. 14 (2013) 4242–4282. http://dx.doi.org/10.3390/ijms14024242.
[5] Y.-H.M. Chan, S.G. Boxer, Model membrane systems and their applications, Curr. Opin. Chem. Biol. 11 (2007) 581–587. http://dx.doi.org/10.1016/j.cbpa.2007.09.020.
[6] R. Frkanec, V. Noethig Laslo, B. Vranešić, K. Mirosavljević, J. Tomašić, A spin labelling study of immunomodulating peptidoglycan monomer and adamantyltripeptides entrapped into liposomes, Biochim. Biophys. Acta 1611 (2003) 187–196. http://dx.doi.org/10.1016/s0005-2736(03)00054-3.
[7] A. Štimac, J. Trmčić Cvitaš, L. Frkanec, O. Vugrek, R. Frkanec, Design and syntheses of mono and multivalent mannosyl-lipoconjugates for targeted liposomal drug delivery, Int. J. Pharmaceutics 511 (2016) 44–56. http://dx.doi.org/10.1016/j.ijpharm.2016.06.123.
[8] M. Šekutor, A. Štimac, K. Mlinarić Majerski, R. Frkanec, Synthesis and characterization of liposome incorporated adamantyl aminoguanidines, Org. Biomol. Chem. 12 (2014) 6005–6013. http://dx.doi.org/10.1039/c4ob00592a.
[9] D. Gray, A.J. Mitchell, C.D. Searles, An accurate, precise method for general labeling of extracellular vesicles, Methods 2 (2015) 360–367. http://dx.doi.org/10.1016/j.mex.2015.08.002.

[10] G. Raposo, W. Stoorvogel, Extracellular vesicles: Exosomes, microvesicles, and friends, J. Cell Biol. 200 (2013) 373–383. http://dx.doi.org/10.1083/jcb.201211138.
[11] A. Martins, H. Vieira, H. Gaspar, S. Santos, Marketed marine natural products in the pharmaceutical and cosmeceutical industries: tips for success, Mar. Drugs 12 (2014) 1066–1101. http://dx.doi.org/10.3390/md12021066.
[12] B. David, J.L. Wolfender, D.A. Dias, The pharmaceutical industry and natural products: historical status and new trends, Phytochem. Rev. 14 (2015) 299–315. http://dx.doi.org/10.1007/s11101-014-9367-z.
[13] S. Rosales-Mendoza Sergio (Ed.), Algae-Based Biopharmaceuticals, Springer, 2016, pp. 1–165.
[14] L. Barsanti, P. Gualtieri (Eds.) Algae, CRC Taylor&Francis, 2006, pp. 251–289.
[15] J.E. Ben-Amotz, W. Polle, D.V. Subba Rao, The Alga Dunaliella Biodiversity, Physiology, Genomics and Biotechnology, Science Publishers, New Hampshire, US, 2009, pp. 1–555.
[16] J.C. Quinn, R. Davis, The potentials and challenges of algae based biofuels: a review of the techno-economic, life cycle, and resource assessment modeling, Bioresour. Technol. 184 (2015) 444–452. http://dx.doi.org/10.1016/j.biortech.2014.10.075.
[17] M. Goettel, C. Eing, C. Gusbeth, W. Frey, Pulsed electric field assisted extraction of intracellular valuables from microalgae, Algal Research 2 (2013) 401–408. http://dx.doi.org/10.1016/j.algal.2013.07.004.
[18] T. Niederwieser, P. Kociolek, A. Hoehn, D. Klaus, Effect of altered nitrogen partial pressure on Chlorellaceae for spaceflight applications, Algal Res.-Biomass Biofuels Bioprod. 41 (2019) 101543–101554. http://dx.doi.org/10.1016/j.algal.2019.101543.
[19] I. Wagner, M. Braun, K. Slenzka, C. Posten, Photobioreactors in Life Support Systems Microalgae biotechnology, in: C. Posten, S.F. Chen (Eds.), Book Series: Advances in Biochemical Engineering-Biotechnology, 153, Springer, 2016, pp. 143–184. http://dx.doi.org/10.1007/10_2015_327.
[20] M. Oren-Shamir, U. Pick, M. Avron, Plasma membrane potential of the alga Dunaliella, and its relation to osmoregulation, Plant Physiol. 93 (1990) 403–408. http://dx.doi.org/10.1104/pp.93.2.403.
[21] F. Pillet, E. Dague, J. Pečar Ilić, I. Ružić, M.-P. Rols, N. Ivošević DeNardis, Changes in nanomechanical properties and adhesion dynamics of algal cells during their growth, Bioelectrochemistry 128 (2019) 154–162. http://dx.doi.org/10.1016/j.bioelechem.2019.02.011.
[22] N. Ivošević DeNardis, J. Pečar Ilić, I. Ružić, N. Novosel, T. Mišić Radić, A. Weber, D. Kasum, Z. Pavlinska, R.K. Balogh, H. Balint, A. Marček Chorvátová, B. Gyurcsik, Algal cell response to laboratory-indeced cadmium stress: a multimethod approach, Eur. Biophys. J. 48 (2019) 124–142. http://dx.doi.org/10.1007/s00249-019-01347-6.
[23] T.C.-C. Jokela, Outer Membrane of Dunaliella tertiolecta: Isolation and Properties, PhD Thesis, University of California, 1969.
[24] R.R.L. Guillard, Culture of Phytoplankton for Feeding Marine Invertebrates, in: Culture of Marine Invertebrate Animals, Springer, Boston, MA, 1975, pp. 29–60. https://doi.org/10.1007/978-1-4615-8714-9_3.
[25] A. Moscho, O. Orwar, D.T. Chiu, B.P. Modi, R.N. Zare, Rapid preparation of giant unilamellar vesicles, Proc. Natl. Acad. Sci. USA 93 (1996) 11443–11447. http://dx.doi.org/10.1073/pnas.93.21.11443.
[26] G. Pletikapić, A. Berquand, T. Mišić Radić, V. Svetličić, Quantitative nanomechanical mapping of marine diatom in seawater using peak force tapping atomic force microscopy, J. Phycol. 48 (2012) 174–185. http://dx.doi.org/10.1111/j.1529-8817.2011.01093.x.
[27] N.R. Baker, Chlorophyll fluorescence: a probe of photosynthesis in vivo, Annu. Rev. Plant Biol. 59 (2008) 89–113. http://dx.doi.org/10.1146/annurev.arplant.59.032607.092759.
[28] S. Takaichi, Carotenoids in algae: distributions, biosyntheses, and functions, Mar. Drugs 9 (2011) 1101–1118. http://dx.doi.org/10.3390/md9061101.
[29] A.L. Chagas, A.O. Rios, A. Jarenkow, N.R. Marcílio, M.A.Z. Ayub, R. Rech, Production of carotenoids and lipids by Dunaliella tertiolecta using CO2 from beer fermentation, Process Biochem. 50 (2015) 981–988. http://dx.doi.org/10.1016/j.procbio.2015.03.012.
[30] J.A. Neilson, D.G. Durnford, Structural and functional diversification of the light-harvesting complexes in photosynthetic eukaryotes, Photosyn. Res. 106 (2010) 57–71. http://dx.doi.org/10.1007/s11120-010-9576-2.
[31] D.M.M. Kleinegris, M.A. van Es, M. Janssen, W.A. Brandenburg, R.H. Wijffels, Carotenoid fluorescence in Dunaliella salina, J. Appl. Phycol. 22 (2010) 645–649. http://dx.doi.org/10.1007/s10811-010-9505-y.
[32] M. Maeda, G.A. Thompson, On the mechanism of rapid plasma membrane and chloroplast envelope expansion in Dunaliella salina exposed to hypoosmotic shock, J. Cell Biol. 102 (1986) 289–297. http://dx.doi.org/10.1083/jcb.102.1.289.
[33] K.J. Einspahr, M. Maeda, G.A. Thompson, Concurrent changes in Dunaliella salina ultrastructure and membrane phospholipid metabolism after hyperosmotic shock, J. Cell Biol. 107 (1988) 529–538. http://dx.doi.org/10.1083/jcb.107.2.529.
[34] J.G. Moloughney, N. Weisleder, Poloxamer 188 (p188) as a membrane resealing reagent in biomedical applications, Recent Pat. Biotechnol. 6 (2012) 200–211. http://dx.doi.org/10.2174/1872208311206030200.
[35] M.A. Borowitzka, L.J. Borowitzka, Dunaliella, in: M.A. Borowitzka, L.J. Borowitzka (Eds.), Micro-Algal Biotechnology, Cambridge University Press, Cambridge, UK, 1988, p. 27.
[36] N. Ivošević DeNardis, J. Pečar Ilić, I. Ružić, G. Pletikapić, Cell adhesion and spreading at a charged interface: Insight into the mechanism using surface techniques and mathematical modelling, Electrochim. Acta 176 (2015) 743–754. http://dx.doi.org/10.1016/j.electacta.2015.07.068.
[37] A. Katz, P. Waridel, A. Shevchenko, U. Pick, Salt-induced changes in the plasma membrane proteome of the halotolerant alga Dunaliella salina as revealed by blue native gel electrophoresis and nano-LC-MS/MS analysis, Mol. Cell. Proteomics 6 (2007) 1459–1472. http://dx.doi.org/10.1074/mcp.m700002-mcp200.
[38] S.W. Jeffrey, E. Skarstad Egeland, Pigments of green and red forms of Dunaliella, and related Chlorophytes, in: A. Ben-Amotz, J. Polle, D. Subba Rao (Eds.), The Alga Dunaliella, Science Publishers, 2009, pp. 111–145. http://hdl.handle.net/102.100.100/118519?index=1.
[39] P. Gueda, R. Rodriguew, L. Loureiro, R. Pereira, B. Fernandes, J.A. Teixeira, V. Vasconcelos, A.A. Cicente, Electrotechnologies applied to microalgal biotechnology – Applications, techniques and future trends, Renew. Sust. Energy Rev. 94 (2018) 656–668. http://dx.doi.org/10.1016/j.rser.2018.06.059.
[40] H. Mendoza, A. Martel, M. Jimenez del Rio, G. Garcia Reina, Oleic acid is the main fatty acid related with carotenogenesis in Dunaliella salina, J. Appl. Phycol. 11 (1999) 15–19. http://dx.doi.org/10.1007/978-94-011-4449-0_65.
[41] B. Gabriel, J. Teissié, Direct observation in the millisecond time range of fluorescent molecule asymmetrical interaction with the electropermeabilized cell membrane, Biophys. J. 73 (1997) 2630–2637. http://dx.doi.org/10.1016/s0006-3495(97)78292-4.
[42] J.R. Lakowicz, Principles of Fluorescence Spectroscopy, Springer, New York, 2010, pp. 1–9.
[43] T. Katsu, T. Imakura, K. Komagoe, K. Masuda, T. Mizushima, Simultaneous measurements of K+ and calcein release from liposomes and the determination of pore size formed in a membrane, Anal. Sci. 23 (2007) 517–522. http://dx.doi.org/10.2116/analsci.23.517.
[44] B. Maherani, E. Arab-Tehrany, A. Kheirolomoom, D. Geny, M. Linder, Calcein release behavior from liposomal bilayer; influence of physicochemical/mechanical/structural properties of lipids, Biochimie 95 (2013) 2018–2033. http://dx.doi.org/10.1016/j.biochi.2013.07.006.
[45] B. Maherani, E. Arab-Tehrany, E. Rogalska, B. Korchowiec, A. Kheirolomoom, M. Linde, Vibrational, calorimetric, and molecular conformational study on calcein interaction with model lipid membrane, J. Nanopart. Res. 15 (2013) 1792–1809. http://dx.doi.org/10.1007/s11051-013-1792-1.
[46] E. Neumann, K. Toensing, S. Kakorin, P. Budde, J. Freym, Mechanism of Electroporative Dye Uptake by Mouse B Cells, Biophys. J. 74 (1998) 98–108. http://dx.doi.org/10.1016/s0006-3495(98)77771-9.
[47] E.B. Sözer, C.F. Pocetti, P.T. Vernier, Asymmetric patterns of small molecule transport after nanosecond and microsecond electropermeabilization, J. Membrane Biol. 25 (2018) 197–210. http://dx.doi.org/10.1007/s00232-017-9962-1.
[48] E.B. Sözer, C.F. Pocetti, P.T. Vernier, Transport of charged small molecules after electropermeabilization — drift and diffusion, BMC, Biophysics 11 (2018) 4–15. http://dx.doi.org/10.1186/s13628-018-0044-2.
[49] R. Dimova, Giant vesicles: a biomimetic tool for membrane characterization, Advances in Planar Lipid Bilayers and, Liposomes 16 (2012) 1–50. https://doi.org/10.1016/B978-0-12-396534-9.00001-5.
[50] R. Dimova, Giant vesicles and their use in assays for assessing membrane phase state, curvature, mechanics and electrical properties, Annu. Rev. Biophys. 48 (2019) 93–119. http://dx.doi.org/10.1146/annurev-biophys-052118-115342.
[51] G. Mao, X. Liang, K.Y. Simon Ng, Direct force measurement of liposomes by atomic force microscopy, in: A. JamesSchwarz, Edward SergeyLyshevski, I. CristianContescu (Eds.), Dekker Encyclopedia of Nanoscience and Nanotechnology, Seven Volume Set, CRC Press, 2004, pp. 933–942. http://citeseerx.ist.psu.edu/viewdoc/download?doi=10.1.1.514.8266&rep=rep1&type=pdf.
[52] I. Ružić, N. Ivošević DeNardis, J. Pečar-Ilić, Kinetics of the liposome adhesion on a mercury electrode: testing of a mathematical model, Int. J. Electrochem. Sc. 4 (2009) 787–793.
[53] N. Ivošević DeNardis, I. Ružić, J. Pečar Ilić, S. El Shawish, P. Ziherl, Reaction kinetics and mechanical models of liposome adhesion on charged interface, Bioelectrochemistry 88 (2012) 48–56. http://dx.doi.org/10.1016/j.bioelechem.2012.05.003.
[54] T. Portet, C. Favard, J. Teissie, D.S. Deanb, M.-P. Rols, Insights into the mechanisms of electromediated gene delivery and application to the loading of giant vesicles with negatively charged macromolecules, Soft Matter 7 (2011) 3872–3881. http://dx.doi.org/10.1039/c0sm01389g.
[55] T. Shimanouchi, H. Ishii, N. Yoshimoto, H. Umakoshi, R. Kuboi, Calcein permeation across phosphatidylcholine bilayer membrane: Effects of membrane fluidity, liposome size, and immobilization, Colloids Surf. B Biointerfaces 73 (2009) 156–160. http://dx.doi.org/10.1016/j.colsurfb.2009.05.014.
[56] P.G. de Gennes, Interactions between polymers and surfactants, J. Phys. Chem. 94 (1990) 8407–8413. http://dx.doi.org/10.1021/j100385a010.
[57] D.L. Perrier, A. Vahid, V. Kathavi, L. Stam, L. Rems, Y. Mulla, A. Muralidharan, G. H. Koenderink, M.T. Kreutzer, P.E. Boukany, Response of an actin network in vesicles under electric pulses, Sci. Rep. 9 (2019) 8151–8162. http://dx.doi.org/10.1101/338566.
[58] C.C. Campillo, A.P. Schroder, C.M. Marques, B. Pepin-Donat, Composite gel-filled giant vesicles: Membrane homogeneity and mechanical properties, Mater. Sci. Eng. C 29 (2009) 393–397. http://dx.doi.org/10.1016/j.msec.2008.08.001.